

## Impurity production by the ICRF antennas in JET

A. Czarnecka<sup>1</sup>, V. Bobkov<sup>2</sup>, I. H. Coffey<sup>3</sup>, L. Colas<sup>4</sup>, A. C. A. Figueiredo<sup>5</sup>, P. Jacquet<sup>6</sup>,  
K. D. Lawson<sup>6</sup>, E. Lerche<sup>7</sup>, M.-L. Mayoral<sup>6</sup>, I. Monakhov<sup>6</sup>, J. Ongena<sup>7</sup>,  
D. Van Eester<sup>7</sup>, K.-D. Zastrow<sup>6</sup> and JET-EFDA contributors\*

*JET-EFDA, Culham Science Centre, Abingdon, OX14 3DB, UK*

<sup>1</sup>*Association Euratom-IPPLM, Hery 23, 01-497 Warsaw, Poland*

<sup>2</sup>*Max-Planck-Institut für Plasmaphysik, EURATOM-Assoziation, D-85748 Garching, Germany*

<sup>3</sup>*Department of Physics, Queen's University, Belfast, BT7 1NN, Northern Ireland, UK*

<sup>4</sup>*CEA, IRFM, F-13108 Saint-Paul-lez-Durance, France*

<sup>5</sup>*Associação EURATOM/IST, Instituto de Plasmas e Fusão Nuclear – Laboratório Associado, Instituto Superior Técnico, P-1049-001 Lisboa, Portugal*

<sup>6</sup>*Euratom/CCFE Association, Culham Science Centre, Abingdon, OX14 3DB, UK*

<sup>7</sup>*Association "EURATOM - Belgian State", ERM-KMS, TEC Partner, Belgium*

### 1. INTRODUCTION

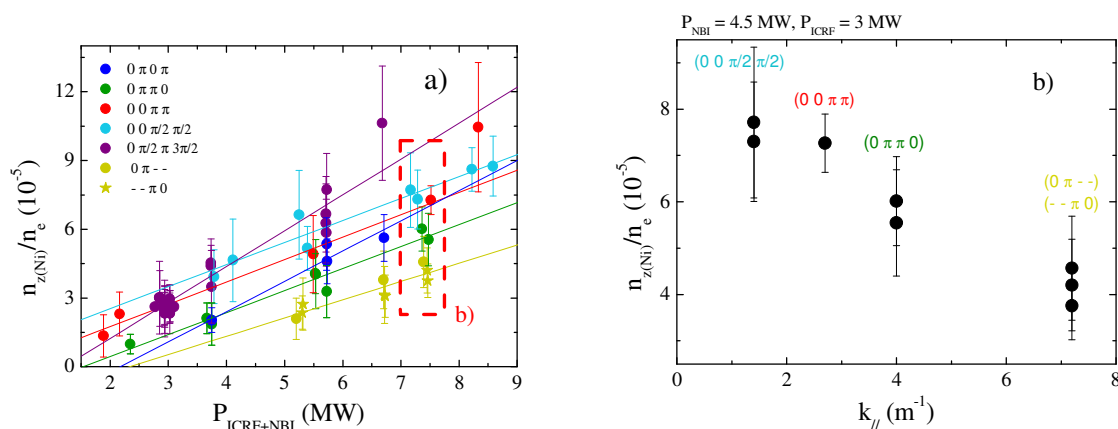
Studying the behaviour of impurities is important to understand and minimize their effects on tokamak plasma performance. A possible source of impurities is the use of Ion Cyclotron Resonance Frequency (ICRF) power. Although this phenomenon can be minimized by improved antenna design [1], recent development on impurities content monitoring can be used to further investigate the processes leading to this increase. More specifically, spectroscopic studies have been recently undertaken on JET in order to monitor the impurity content during the operation of the A2 ICRF antennas. In this paper, Nickel (Ni) release during ICRF heating is presented as a function of the relative phasing of the antenna straps, D2 gas injection level, plasma-strap distance, and applied ICRF power level.

### 2. EXPERIMENTAL ARRANGEMENT AND ANALYSIS METHOD

The behaviour of the Ni impurity concentration, expressed as the ratio of impurity density to electron density, has been studied by monitoring the Ni XXVI line at 165.04 Å with a midplane-viewing survey SPRED spectrometer, known at JET as the KT2 diagnostic [2, 3]. This spectrometer typically registers VUV spectra in the wavelength range of 100–1100 Å with an approximate spectral resolution of 5 Å. A method based on the combination of absolutely calibrated VUV transition intensity measurements with Universal Transport Code (UTC) simulations [4] has been used to analyse the spectroscopic data, whereby impurity densities have been determined for JET discharges. In this method, the VUV line intensity for Li-like transitions in Ni is reproduced with UTC for a wide class of transport coefficients. From the dependence of the ratio between the derived impurity densities and the line intensity on local electron temperature, a linear fit is established allowing the calculation of the local impurity density in the region with normalized radius from 0.5 to 0.6 [4].

## 2. ALTERNATIVE A2 ANTENNA PHASINGS

Changing the relative phasings between the four straps of the A2 antennas modifies the spectrum of parallel wave number  $k_{\parallel}$ , resulting in different ICRF absorption by the plasma. Discharges with “dipole” ( $0\pi 0\pi$ ), “symmetric dipole” ( $0\pi\pi 0$ ), “super dipole” ( $00\pi\pi$ ), “super current-drive” ( $00\pi/2\pi/2$ ), ( $0\pi/2\pi 3\pi/2$ ), only 2 antenna straps powered ( $--\pi 0$ ), and ( $0\pi--$ ) phasings have been compared. Experiments were performed in L-mode with magnetic field  $B_T = 3$  T, plasma current  $I_p = 2$  MA, and an antenna-separatrix distance of  $11.0 \pm 0.5$  cm. Minority hydrogen ICRF heating at  $f = 42$  MHz in D plasma has been applied in all pulses. The ICRF power has been changed by steps up to 4 MW, and NBI power up to 4.5 MW has been applied. The proportion of ICRF to NBI power has been changed for the analysed pulses, but previous studies showed that the Ni content is not affected by the NBI power level [4].



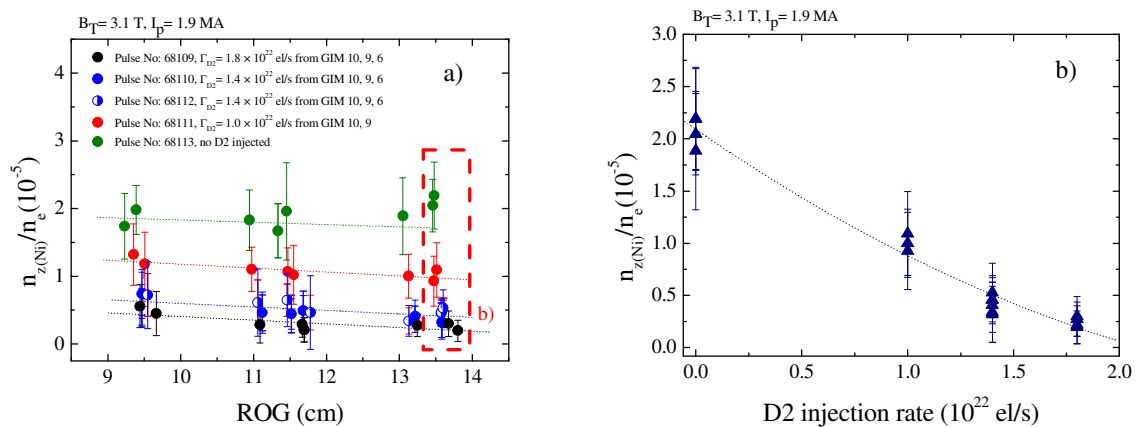
**Figure 1.** a) Correlation between Ni concentration ( $r/a \approx 0.5-0.6$ ) and total applied heating power for different A2 antenna phasings, and b) Nickel concentration vs parallel wave number  $k_{\parallel}$  for selected points in a) with 3 MW of ICRF power and 4.5 MW of NBI.

Figure 1a) shows the correlation between Ni concentration and total applied heating power for different A2 antenna phasings, which are characterized by different  $k_{\parallel}$  spectra. It can be observed that for antenna phasings with higher dominant  $k_{\parallel}$ , the Ni impurity concentration was reduced in the central part of the plasma ( $r/a \approx 0.5-0.6$ ). This behaviour can be related to a lower electric field on the antenna structure [1] — the main source of Ni is thought to be due to the acceleration of edge particles in the antenna-near-field toward structures close to the antennas and support the fact that for low  $k_{\parallel}$  the heating efficiency is low [5] and the part of the total ICRF injected power, not absorbed in the plasma core is remaining in the edge, and thus increases the radiation losses.

## 3. EFFECT OF D2 GAS INJECTION ON Ni PRODUCTION

Nickel concentration has also been monitored during experiments performed in H-mode that aimed at improving the ICRF coupling at large antenna strap-separatrix distances — up to 19 cm — by

injecting gas from different inlets [6]. The first set of experiments was performed in the ITER-AT configuration (lower triangularity  $\delta_l \approx 0.50$ , upper triangularity  $\delta_u \approx 0.38$ ), characterised by very high recycling and very low amplitude / high frequency type I ELMs. The magnetic field was  $B_T = 3.1$  T, plasma current was  $I_p = 1.9$  MA, and central electron density was  $n_e \approx 5 \times 10^{19} \text{ m}^{-3}$ . To reach H-mode 16 MW of NBI power were applied, while the used ICRF heating scheme was hydrogen (H) minority heating in D plasma with an ICRF frequency of 47 MHz and a “ $0\pi 0\pi$ ” antenna phasing. To obtain an ITER-relevant antenna-LCFS distance, values of the Radial Outer Gap (ROG) have been scanned from 10 to 14 cm. Gas injector module (GIM) GIM 6, which is located in the midplane near the ICRF antenna B, as well as GIM 9 and GIM 10, which are situated in the divertor have been used to inject D2 into the plasma. It can be observed in Figure 2 that Ni concentration decreases with ROG, and also with the D2 injection rate. Note that the ICRF coupling also decreases with ROG but increases with gas puff [6].



**Figure 2.** a) Correlation between Ni concentration ( $r/a \approx 0.5$ – $0.6$ ) and antenna–separatrix distance ROG, and b) Ni concentration ( $r/a \approx 0.5$ – $0.6$ ) vs different levels of injected D2 gas for selected points in a) with ROG around 14 cm (ITER-AT configuration).

The reduction of the Ni content with gas puffing might be due to a change in temperature and density, modifications in flow and transport [7], or impurity energy alterations in the SOL — a key factor for sputtering yield.

The second set of experiments was performed in the HT3 configuration (lower triangularity  $\delta_l \approx 0.35$ , upper triangularity  $\delta_u \approx 0.45$ ) for which recycling is very low and characteristic type I ELMs with very high amplitude and low frequency are present. In the experiments, the following parameters were used: magnetic field  $B_T = 1.55$  T, plasma current  $I_p = 1.5$  MA, and central electron density  $n_e \approx 6 \times 10^{19} \text{ m}^{-3}$ . 8 MW of NBI power have been applied. The used ICRF heating scheme was 2nd harmonic H minority heating in D plasma with an ICRF frequency of 47 MHz and a “ $0\pi 0\pi$ ” antenna phasing. The GIMs used to inject D2 were GIM 2 and GIM6 (midplane), GIM 8 (top), and GIM 9 (divertor).

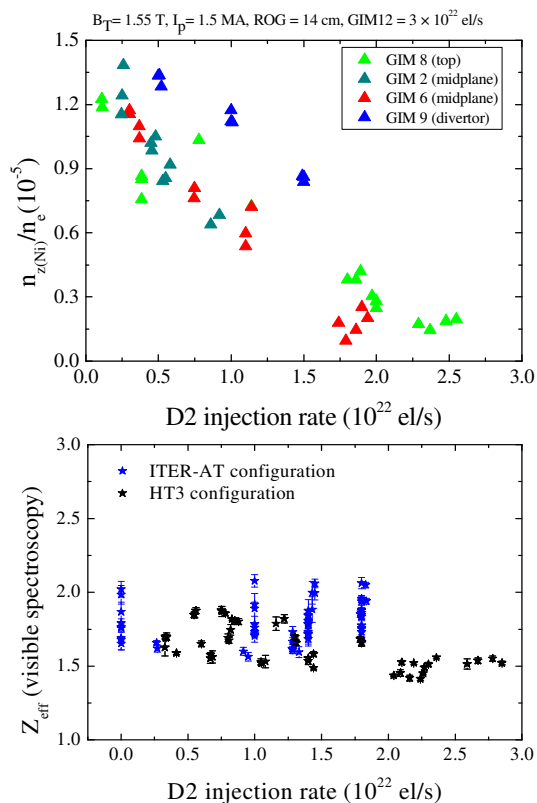


**Figure 3.** Effect on Ni concentration of D2 gas injection using different GIMs (HT3 configuration).

**Figure 4.**  $Z_{\text{eff}}$  vs D2 gas injection rate for all points presented in Figure 2a and 3.

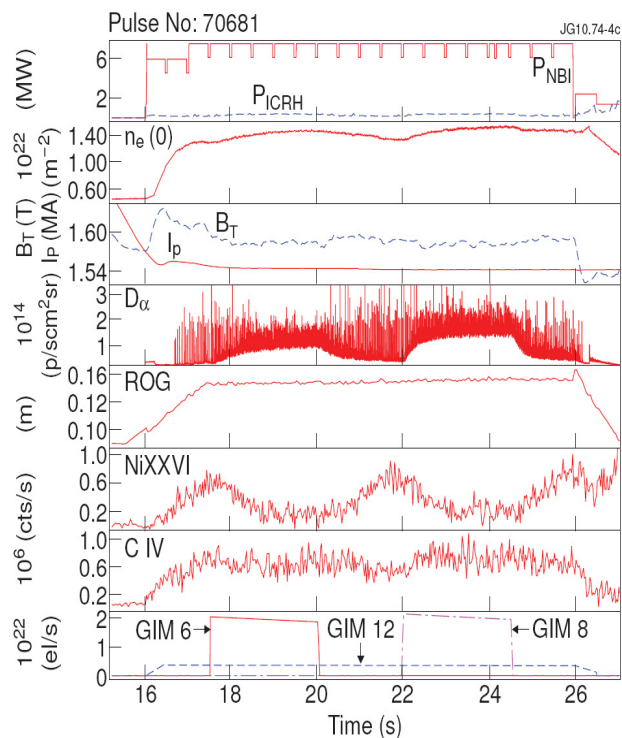


**Figure 5.** Time evolutions of the main plasma parameters for typical shot in HT3 configuration.

Similarly to previous set of experiments for higher gas injection rates, although  $n_e$  in the scrape-off layer (SOL) increased and the coupling improved, the Ni concentration decreased. Interestingly, the actual location of gas injection was found to impact on both coupling [6] and Ni concentration — see Figure 3, this effect being currently further documented. The relative changes observed in Ni (both ITER-AT and HT3 configuration) when changing the gas injection rate are larger than the relative changes in  $Z_{\text{eff}}$  and C (see Figure 4 and 5) suggesting that the source of Ni is local to the antennas.

## ACKNOWLEDGMENTS

This work was supported by EURATOM and carried out within the framework of the European Fusion Development Agreement. The views and opinions expressed herein do not necessarily reflect those of the European Commission.

- [1] V. Bobkov *et al.*, Nucl. Fusion **50**, 035004 (2010)
  - [2] I. H. Coffey *et al.*, Rev. Sci. Instrum. **75**, 3737 (2004)
  - [3] K. D. Lawson *et al.*, JINST **4** P04013 (2009)
  - [4] A. Czarnecka *et al.*, 36th EPS Conference ECA vol. **33E** P-2.146 (2009)
  - [5] E. Lerche *et al.*, in RF Power in Plasmas, AIP Conf. Proc. **1187** (2009), Melville, New York, 2009, p93
  - [6] M.-L. Mayoral *et al.*, in RF Power in Plasmas, AIP Conf. Proc. **933** (2007), Melville, New York, 2007, p55
  - [7] P. Belo *et al.*, Plasma Phys. Control. Fusion **46** (2004) 1299
- \* See the Appendix of F. Romanelli *et al.*, Proceedings of the 22nd IAEA Fusion Energy Conference, Geneva, Switzerland, 2008